GEOLOGY | THE GEOLOGICAL SOCIETY OF AMERICA®

https://doi.org/10.1130/G48930.1

Manuscript received 8 February 2021
Revised manuscript received 6 May 2021
Manuscript accepted 18 May 2021

Published online 15 July 2021

Staged formation of the supergiant Olympic Dam uranium deposit, Australia

Kathy Ehrig[1,2], Vadim S. Kamenetsky[2]*, Jocelyn McPhie[2], Edeltraud Macmillan[1], Jay Thompson[2], Maya Kamenetsky[2] and Roland Maas[3]

[1]BHP Olympic Dam, Adelaide, SA 5000, Australia
[2]School of Natural Sciences, University of Tasmania, Hobart, TAS 7001, Australia
[3]School of Earth Sciences, University of Melbourne, Melbourne, VIC 3010, Australia

ABSTRACT

The origins of many supergiant ore deposits remain unresolved because the factors responsible for such extreme metal enrichments are not understood. One factor of critical importance is the timing of mineralization. However, timing information is commonly confounded by the difficulty of dating ore minerals. The world's largest uranium resource at Olympic Dam, South Australia, is exceptional because the high abundance of U allows U-Pb dating of ore minerals. The Olympic Dam U(-Cu-Au-Ag) ore deposit is hosted in ca. 1.59 Ga rocks, and the consensus has been that the supergiant deposit formed at the same time. We argue that, in fact, two stages of mineralization were involved. Paired *in situ* U-Pb and trace element analyses of texturally distinct uraninite populations show that the supergiant size and highest-U-grade zones are the result of U addition at 0.7–0.5 Ga, at least one billion years after initial formation. This conclusion is supported by a remarkable clustering of thousands of radiogenic $^{207}Pb/^{206}Pb$ model ages of Cu sulfide grains at this time. Upgrading of the original ca. 1.59 Ga U deposit to its present size at 0.7–0.5 Ga may have resulted from perturbation of regional fluid flow triggered by global climatic (deglaciation) and tectonic (breakup of Rodinia) events.

INTRODUCTION

Since the discovery of the supergiant Olympic Dam Cu-U-Au-Ag deposit (South Australia) in 1975, neither its size (e.g., 11.1 Gt of ore, including 2.6 Mt of U_3O_8; BHP, 2020) nor the diversity of metals and minerals have been adequately explained. Although Olympic Dam is regarded as a type example of an iron oxide–copper–gold deposit (IOCG; Hitzman et al., 1992), fundamental questions regarding metal and fluid sources and age(s) of these sources and related mineralization have remained unanswered, possibly because current thinking links ore formation to a single tectonic-magmatic event, the emplacement of the Gawler silicic large igneous province (LIP) at ca. 1.59 Ga (Johnson and Cross, 1995; Allen et al., 2008; McPhie et al., 2011b; Ciobanu et al., 2013; Cherry et al., 2018; Courtney-Davies et al., 2020).

Most of the U at Olympic Dam is present in uraninite, brannerite, and coffinite, whereas the main Cu minerals are chalcopyrite, bornite, and chalcocite (Ehrig et al., 2018, 2012). The U minerals and Cu sulfides are fine grained, disseminated, and closely associated with abundant hematite. These minerals occur within the Olympic Dam Breccia Complex (ODBC; Reeve et al., 1990), which has an area of ~6 km × 3 km (Fig. 1) and thickness in the range 500 m to >1000 m. The ODBC occurs within the undeformed A-type Roxby Downs Granite (1593.87 ± 0.21 Ma; Cherry et al., 2018). The age and contact relationships of the Roxby Downs Granite suggest that it intruded the overlying, broadly comagmatic Gawler Range Volcanics (1594.73 ± 0.30 Ma; Cherry et al., 2018).

The most common clast type in the breccia complex is Roxby Downs Granite. The texture, contact relationships, distribution, and nonstratified character of breccias in the ODBC are consistent with subsurface fragmentation of already solid granite involving a combination of tectonic and hydrothermal processes (Oreskes and Einaudi, 1990; Reeve et al., 1990; McPhie et al., 2011a). Large domains in the center of the ODBC also include clasts of the Gawler Range Volcanics and younger bedded clastic facies (1590.97 ± 0.58 Ma; Cherry et al., 2018). Granitoid detritus in the bedded clastic facies was probably derived from the Roxby Downs Granite, requiring partial exhumation of the granite before ca. 1591 Ma (Cherry et al., 2018), most likely during the ~3 m.y. gap between emplacement of the granite and deposition of the bedded clastic facies.

Some uraninite in the ODBC was formed ca. 1.59 Ga (e.g., Ciobanu et al., 2013; Macmillan et al., 2016b; Apukhtina et al., 2017), but younger ages have also been recorded (Trueman et al., 1988; Johnson, 1993; Macmillan et al., 2016b). In addition, resource estimates for U and total Pb suggest that the U mineralization in its present form may be larger than it was at 1.59 Ga: U and Pb distributions do not show consistent spatial correlations (Fig. 1), and the U/Pb ratio (by weight) is 4.5, higher than the ratio of 3.8 expected if all U was in place at 1.59 Ga, producing radiogenic Pb in a closed system. Some of the Pb is common and/or thorogenic in origin, which increases the discrepancy. Notably, the highest grades of the U ore have U/Pb ratios >10 (Fig. 2), indicating pronounced Pb deficits in parts of the ODBC (Fig. 1). This relationship suggests that either a large fraction of uranogenic Pb was lost or more U was added long after initial U mineralization at 1.59 Ga. Lead loss would result in complementary radiogenic Pb enrichment elsewhere in the district, but no such Pb repositories have been identified to date. The timing of U deposition is thus critical because current ore-genesis and exploration models do not recognize the possibility of post–1.59 Ga U addition.

TWO TYPES AND AGES OF URANINITE

Uraninite, coffinite, and brannerite contain >85% of the U present and are disseminated in

*E-mail: dima.kamenetsky@utas.edu.au

CITATION: Ehrig, K., et al., 2021, Staged formation of the supergiant Olympic Dam uranium deposit, Australia: Geology, v. 49, p. 1312–1316, https://doi.org/10.1130/G48930.1

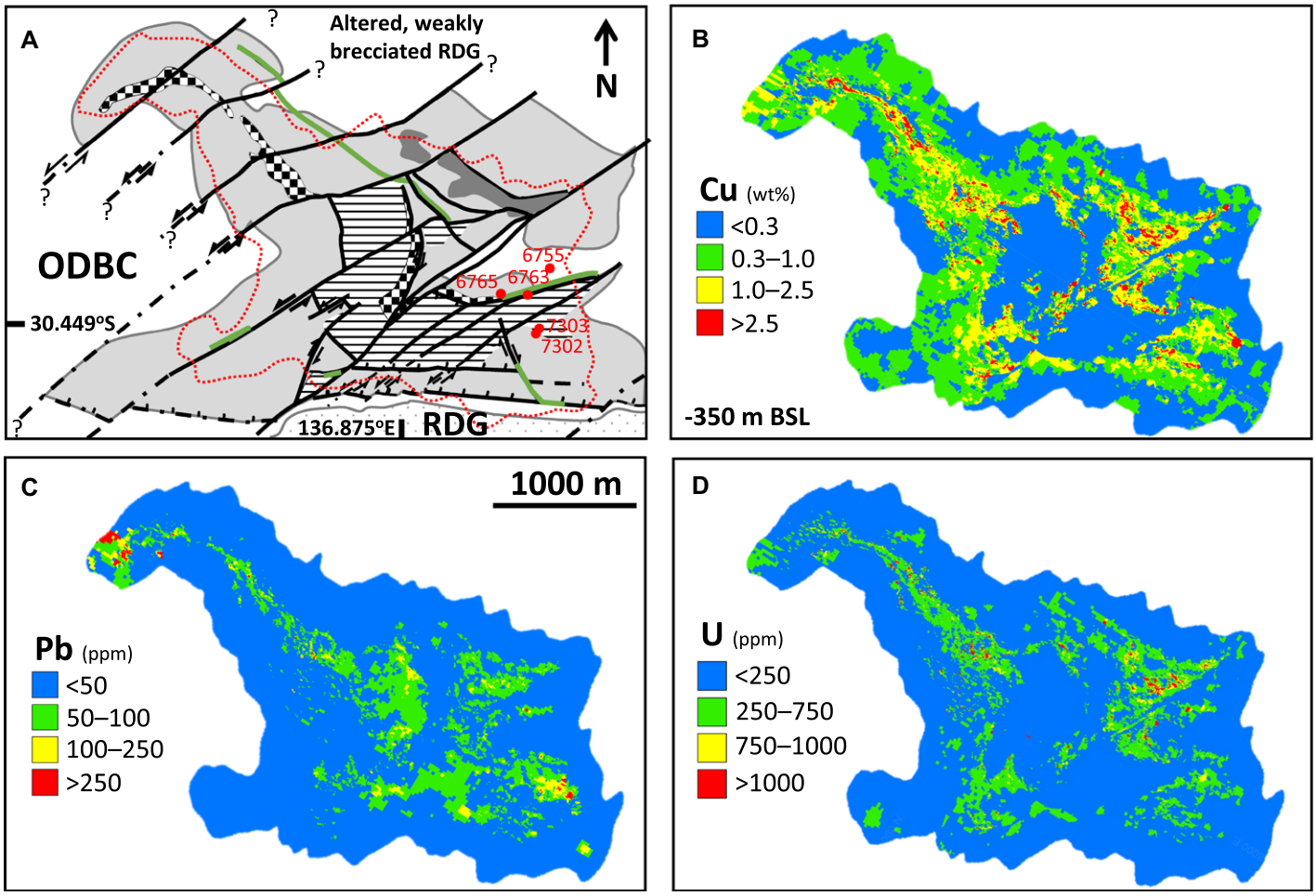

Figure 1. Geological and Cu-Pb-U distribution maps of the Olympic Dam deposit in South Australia. (A) Simplified geological plan of the deposit showing Roxby Downs Granite (RDG), Olympic Dam Breccia Complex (ODBC), granite-rich breccia (<5 wt% Fe, pale gray color on map), granite- to hematite-rich breccias (5–25 wt% Fe, dark gray), hematite-rich breccias (>25 wt% Fe, chess pattern), variably altered bedded clastic facies (horizontal lines), mafic and/or ultramafic dikes (green lines), and locations of five uraninite-bearing samples that were used for geochronology in this study (red dots). Lines represent faults. The publicly declared mineral resource (BHP, 2020) is enclosed by red dotted outline (see Item S1 [see footnote 1] for more details). (B–D) Cu-Pb-U distribution maps within the resource outline, located at a depth of 350 m below sea level (BSL). Uranium has high spatial correlation with Cu but is partially decoupled from Pb.

sulfide and gangue minerals (Ehrig et al., 2012); the remaining 15% of U is hosted in other minerals, notably hematite (Oreskes and Einaudi, 1990; Ciobanu et al., 2013). The major textural types of uraninite are (1) euhedral grains <30 μm in size ("class 1 primary uraninite"; Macmillan et al., 2016b) and (2) subhedral to round grains (<30 to ~100 μm), which form larger aggregates and fill veinlets as much as 1 mm wide (Figs. 2 and 3B). The latter are prominent in high-grade ore zones and are equivalent to "class 4 massive uraninite" (Macmillan et al., 2016b).

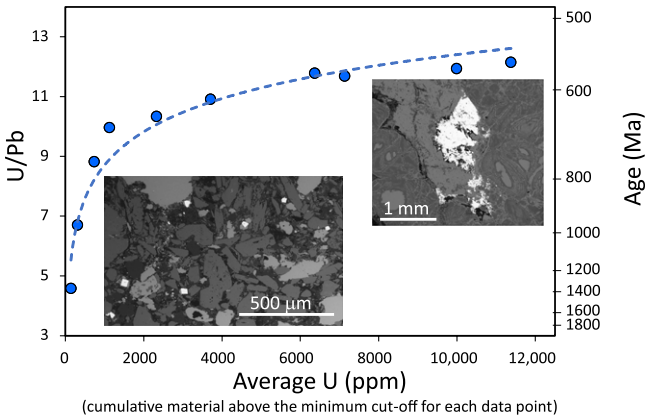

Figure 2. Relationship of total U/Pb ratio (by weight) and average U concentration of binned resource block model grades throughout the Olympic Dam (South Australia) orebody. Much of the U is present in rocks with <1000 ppm U, where U primarily occurs as "class 1" euhedral uraninite grains (visible as small bright areas in scanning electron microscopy–backscattered electron [SEM-BSE] image on the left). Ores with higher U grades (>1000 ppm) are characterized by U/Pb of 9–12, equivalent to "chemical" U-Pb ages in the range 0.7–0.55 Ga (for information on chemical U-Pb ages, see Item S1 in the Supplemental Material [see footnote 1]). The dominant form of uraninite in these high-U rocks is non-euhedral uraninite (the "class 4" uraninite of Macmillan et al., 2016b; bright areas in SEM-BSE image on the right). Chemical U/Pb ages on the right are calculated assuming Th/U = 0 (see Item S1).

Uranium-lead dating of fine-grained euhedral uraninite yielded ages ca. 1.59 Ga, such as the 1588 ± 4 Ma suite shown in Figure 3A, consistent with other U-Pb ages for fine-grained euhedral uraninite associated with early U mineralization (Macmillan et al., 2016b; Apukhtina et al., 2017). The euhedral uraninite grains have high total rare earth element (REE) contents, relatively unfractionated REE patterns with low Ce/Lu and pronounced La and Eu depletions, and low Y/Ho (Fig. 3B). In contrast, texturally distinct non-euhedral uraninite grains have variably preserved U-Pb ages near 0.5 Ga (532 ± 7 and 474 ± 4 Ma; Fig. 3A), and are characterized by lower total REE contents and REE patterns with very low La/Sm, pronounced peaks at Sm, and a lack of Eu anomalies (Fig. 3B).

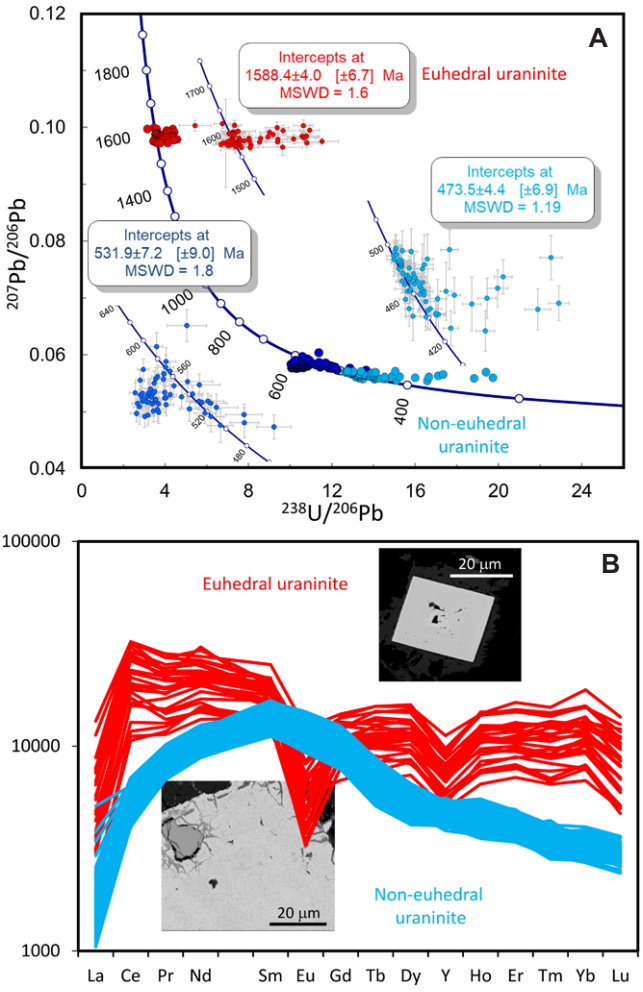

Figure 3. Uranium-lead (U-Pb) dating, textures, and rare earth element (REE) compositions of dominant textural uraninite types preserved at Olympic Dam (South Australia). (A) Tera-Wasserburg U-Pb concordia diagram showing laser ablation–inductively coupled plasma–mass spectrometry U-Pb ages for euhedral and non-euhedral uraninite, equivalent to "class 1" (primary uraninite) and "class 4" (massive uraninite), respectively (Macmillan et al., 2016a, 2016b). Age of 1588 ± 4 Ma for euhedral uraninite (samples RX7302, RX7303) is consistent with U-Pb dates for other "early" mineralization at Olympic Dam (e.g., Ciobanu et al., 2013; Apukhtina et al., 2017). Dated examples of non-euhedral uraninite (e.g., samples RX6755, RX6763, RX6765), a type found primarily in the high-grade U ores but also as overgrowths on older uraninite, yield ages of 532 ± 7 and 474 ± 4 Ma. MSWD—mean squared weighted deviation. (B) Chondrite-normalized REE patterns for the ca. 1.59 Ga and ca. 0.5 Ga uraninites; note the marked differences in total REE contents, shape of patterns, and relative abundances of Eu. Typical textures of these uraninite types are shown as scanning electron microscopy–backscattered electron images in the top right and bottom left of panel B. See Item S2 (see footnote 1) for analytical details, and Tables S1 and S2 for uraninite U-Th-Pb isotope and compositional results, respectively.

LATE NEOPROTEROZOIC–CAMBRIAN URANIUM ADDITION AT OLYMPIC DAM

Evidence from Age and Composition of Uraninite

Since the start of mining at Olympic Dam, assaying of diamond drill core and subsequent resource modeling indicated a deficit of Pb compared to the amount expected in a U deposit formed at 1.59 Ga ("The apparent inconsistency between the pre-mid Proterozoic age of the Olympic Dam copper- uranium- gold mineralization and its overall low lead content…"; Trueman, 1986, p. 2). Our data suggest that mismatched U and Pb abundances in the deposit are best accounted for by at least part of the U having been added late, as late as 1 b.y. after initial formation at ca. 1.59 Ga. The highest U ore grades (>2000 ppm U) are associated with U/Pb ≥ 10, equivalent to "chemical" U-Pb ages <0.7 Ga (Fig. 2). Furthermore, the lack of abundant fission fragments and relatively low inferred neutron fluence in the U ores are more easily reconciled with a Neoproterozoic rather than a Mesoproterozoic U age (Kirchenbaur et al., 2016). These observations are consistent with the presence of the texturally distinct generation of ca. 0.5 Ga uraninite described here (Fig. 3). Uraninite of this age is locally found with partially preserved yet significantly altered remnants of the older (1.59 Ga) euhedral uraninite (Macmillan et al., 2016b), and it dominates the highest U ore grades in the deposit, corroborating the younger "chemical" U-Pb ages (Fig. 2). REE patterns in this uraninite generation, having abundance maxima around Sm-Gd and lacking Eu depletions, are distinct from those in euhedral ca. 1.59 Ga uraninite (Fig. 3B) and resemble REE signatures typical of low-temperature uraninite in the large, high-grade Proterozoic unconformity-related U deposits of Canada and northern Australia (Fryer and Taylor, 1987; Frimmel et al., 2014).

Evidence from Pb Isotopes in Cu Sulfides

Independent evidence for a major U mineralizing event in the late Neoproterozoic to Cambrian is recorded in Pb isotope compositions of hydrothermal Cu sulfides at Olympic Dam. Lead isotope data acquired by laser-ablation inductively coupled plasma mass spectrometry in thousands of chalcopyrite, bornite, and chalcocite grains from across the deposit define trends that record mixing of common Pb with radiogenic Pb characterized by $^{207}Pb/^{206}Pb^*$ in the range 0.07–0.06 (Fig. 4A). U concentrations in these sulfides, including those with highly radiogenic Pb, vary widely, but the vast majority have low U/Pb ratios, implying that radiogenic Pb is "unsupported" (i.e., did not evolve within the low-U sulfide carrier minerals) and inherited from U minerals, a common observation in old U deposits (Gulson and Mizon, 1980; Kister et al., 2004). The timing of production and release of highly radiogenic Pb in U minerals and its capture as "unsupported" radiogenic Pb in Cu sulfides can be constrained using simple modeling with the variables t_1 (time of formation of the U mineral), t_2 (time of release of radiogenic Pb from the U mineral, i.e., capture in sulfides), and the radiogenic $^{207}Pb/^{206}Pb$ inferred from isotopic analyses of the Cu sulfides (see also Item S3 in the Supplemental Material[1]). Varying two of these parameters predicts the third, thus providing model ages that can be compared with other evidence. Unsupported radiogenic Pb with $^{207}Pb/^{206}Pb^*$ of 0.07–0.06 can be produced in U minerals formed in the period 0.9–0.6 Ga if Pb release occurred in the recent geological past ($t_2 = 0$; Fig. 4B). If Pb release occurred earlier, the parental U minerals cannot be older than ca. 0.7 Ga. Destabilization and alteration of U minerals, known from many U deposits (Fayek et al., 1997; Martz et al., 2019), is well documented at Olympic Dam (Macmillan et al., 2016a, 2016b). The remarkably homogeneous and low $^{207}Pb/^{206}Pb^*$ in the Cu sulfide minerals thus implies a major period of U mineral formation at 0.7–0.5 Ga, broadly consistent with the ca. 0.5 Ga ages of non-euhedral uraninite (Fig. 3A). This uraninite population, with its distinct texture and trace element composition (Fig. 3B), could be a remnant or late phase of the U mineralization event(s) preserved in the Pb isotope records of the Cu sulfide minerals. The presence of young (1.59 Ga) radiogenic Pb in the sulfides also implies widespread modification of precursor Cu sulfide minerals and perhaps new sulfide mineral growth concomitant

[1]Supplemental Material. Items S1 (mine-scale maps of Cu, U, Pb grades), S2 (methods), and S3 (interpretation of Pb isotopes in Cu sulfides); and Tables S1 and S2 (U-Pb dating and REE compositions of uraninite, respectively). Please visit https://doi.org/10.1130/GEOL.S.14842710 to access the supplemental material, and contact editing@geosociety.org with any questions.

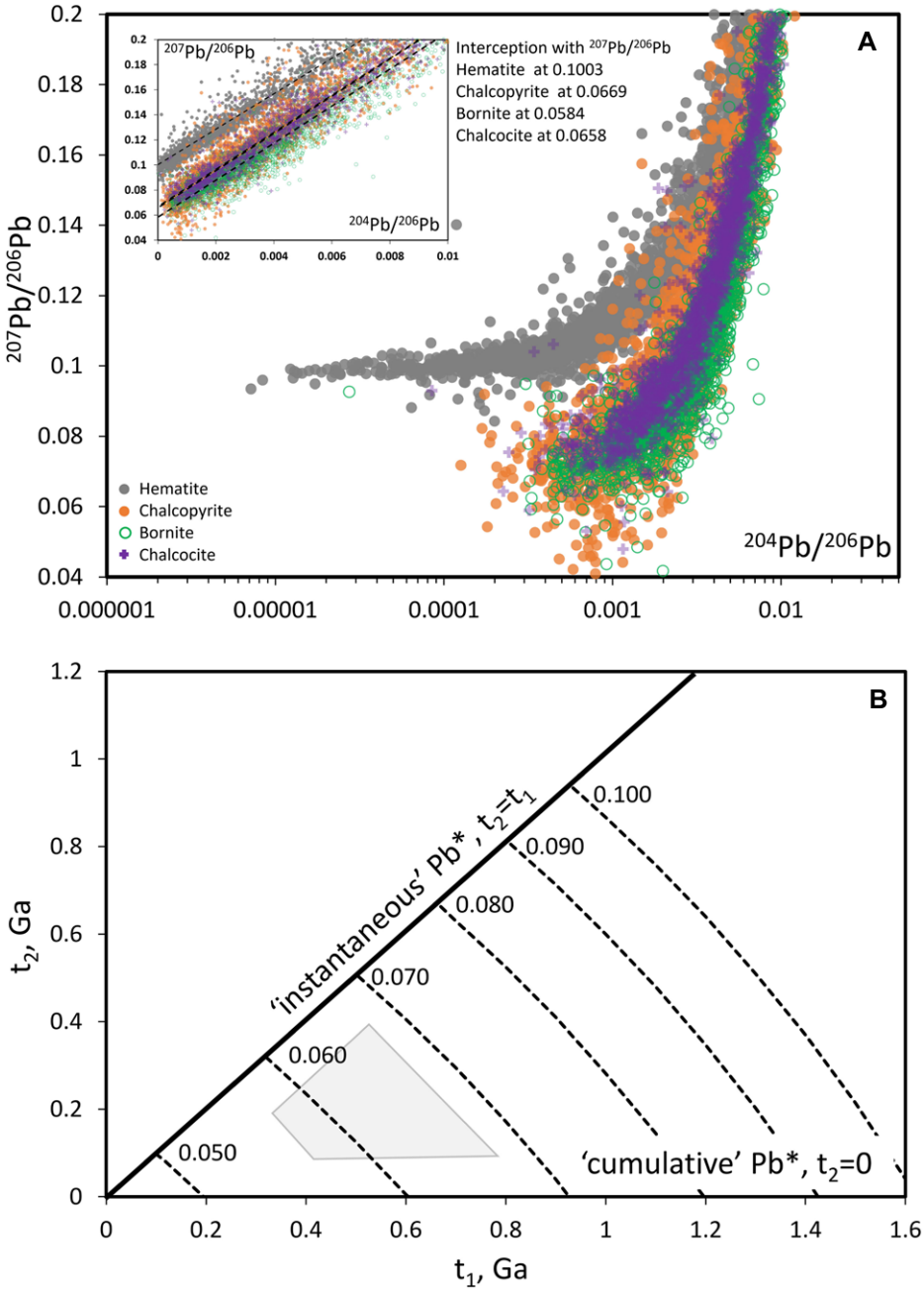

Figure 4. Lead isotope compositions of Olympic Dam (South Australia) Cu sulfides, collected across the entire deposit (i.e., not restricted to areas of high-grade U mineralization). (A) $^{207}Pb/^{206}Pb$ versus log $^{204}Pb/^{206}Pb$ diagram showing data for 7772 Cu sulfide grains (chalcopyrite, bornite, chalcocite; data will be published elsewhere) representative of the orebody. $^{207}Pb/^{206}Pb$ ratios at the lowest common Pb contents ($^{204}Pb/^{206}Pb$ <0.001) are ~0.06, much lower than the radiogenic component inferred for hematite (4909 grains, $^{207}Pb/^{206}Pb^*$ ~0.10). Inset shows same data with linear *x*-axis: regressions of each data set yield *y*-axis intercepts (inferred radiogenic $^{207}Pb/^{206}Pb^*$) of 0.0669, 0.0584, 0.0658, and 0.1003 for chalcopyrite, bornite, chalcocite, and hematite, respectively. All results were obtained by laser ablation–inductively coupled plasma–mass spectrometry. (B) Relationship between $^{207}Pb/^{206}Pb^*$ (diagonal dashed trends), t_1 (age of U mineral formation, *x*-axis), and t_2 (age of Pb* release from its parental U mineral, *y*-axis; for details see Item S3 [see footnote 1]). $^{207}Pb/^{206}Pb^*$ ratios for Cu sulfides centered on 0.006–0.07 (shaded polygon) imply a major period of U mineralization in the late Neoproterozoic–Cambrian followed by transfer of ingrown Pb* as well as pyrite (not shown) some tens to hundreds of million years later.

with this stage of U mineralization. Renewed hydrothermal activity post–1 Ga is also recorded in other minerals at Olympic Dam (Apukhtina et al., 2020; Maas et al., 2020).

Late Neoproterozoic–Cambrian U at Olympic Dam may be linked to global tectonic and climatic events. The ODBC was first exposed prior to deposition of the Mesoproterozoic Pandurra Formation (Cherry et al., 2017) and again prior to deposition of ~350 m of flat-lying Cryogenian and younger sedimentary formations (Drexel et al., 1993). These sedimentary formations were deposited under periglacial conditions during the Marinoan glaciation (Tonkin and Creelman, 1990), part of the global late Neoproterozoic glaciation (Hoffman et al., 2017). The later-stage U at Olympic Dam, broadly constrained here to the period 0.7–0.5 Ga, thus overlapped with Cryogenian glaciation and/or deglaciation and the associated rise in atmospheric oxygen (Lyons et al., 2014). This period also overlaps with the final breakup of the Rodinia supercontinent and early amalgamation of Gondwana (Veevers, 2004; Li et al., 2008). The younger (0.7–0.5 Ga) U mineralization at Olympic Dam may thus have been a result of enhanced mobility of oxidized U in surficial and basinal fluids combined with near-contemporaneous exhumation and shallow burial of the ODBC.

CONCLUSIONS

Our study challenges the existing paradigm of U mineralization at Olympic Dam being a single event the same age as the ca. 1.59 Ga Gawler silicic LIP host rocks. Rather, the existence of texturally and chemically distinct generations of uraninite and evidence from sulfide Pb isotope compositions indicate that U at Olympic Dam is the result of at least two major stages of U deposition, the first at ca. 1.59 Ga and the second broadly constrained to the period 0.7–0.5 Ga. Supergiant U mineralization at Olympic Dam is thus the result of staged accumulation of U in two episodes a billion years apart.

ACKNOWLEDGMENTS

This study was supported by the Australian Research Council Linkage project (grant LP130100438) and BHP Olympic Dam. Jesse Clark and James Taylor are thanked for assistance with the geological map. We are grateful to Liam Courtney-Davies, Kevin Ansdell, and Julio Almeida for insightful reviews and for sharing their knowledge of uranium deposits, and to Marc Norman for editorial handling.

REFERENCES CITED

Allen, S.R., McPhie, J., Ferris, G., and Simpson, C., 2008, Evolution and architecture of a large felsic Igneous Province in western Laurentia: The 1.6 Ga Gawler Range Volcanics, South Australia: Journal of Volcanology and Geothermal Research, v. 172, p. 132–147, https://doi.org/10.1016/j.jvolgeores.2005.09.027.

Apukhtina, O.B., Kamenetsky, V.S., Ehrig, K., Kamenetsky, M.B., Maas, R., Thompson, J., McPhie, J., Ciobanu, C.L., and Cook, N.J., 2017, Early, deep magnetite-fluorapatite mineralization at the Olympic Dam Cu-U-Au-Ag deposit, South Australia: Economic Geology and the Bulletin of the Society of Economic Geologists, v. 112, p. 1531–1542, https://doi.org/10.5382/econgeo.2017.4520.

Apukhtina, O.B., Ehrig, K., Kamenetsky, V.S., Kamenetsky, M.B., Goemann, K., Maas, R., McPhie, J., Cook, N.J., and Ciobanu, C.L.,

2020, Carbonates at the supergiant Olympic Dam Cu-U-Au-Ag deposit, South Australia. Part 1: Distribution, textures, associations and stable isotope (C, O) signatures: Ore Geology Reviews, v. 126, 103775, https://doi.org/10.1016/j.oregeorev.2020.103775.

BHP, 2020, Annual Report 2020: https://www.bhp.com/-/media/documents/investors/annual-reports/2020/200915_bhpannualreport2020.pdf (accessed January 2021).

Cherry, A.R., McPhie, J., Kamenetsky, V.S., Ehrig, K., Keeling, J.L., Kamenetsky, M.B., Meffre, S., and Apukhtina, O.B., 2017, Linking Olympic Dam and the Cariewerloo Basin: Was a sedimentary basin involved in formation of the world's largest uranium deposit?: Precambrian Research, v. 300, p. 168–180, https://doi.org/10.1016/j.precamres.2017.08.002.

Cherry, A.R., Ehrig, K., Kamenetsky, V.S., McPhie, J., Crowley, J.L., and Kamenetsky, M.B., 2018, Precise geochronological constraints on the origin, setting and incorporation of ca. 1.59 Ga surficial facies into the Olympic Dam Breccia Complex, South Australia: Precambrian Research, v. 315, p. 162–178, https://doi.org/10.1016/j.precamres.2018.07.012.

Ciobanu, C.L., Wade, B.P., Cook, N.J., Schmidt Mumm, A., and Giles, D., 2013, Uranium-bearing hematite from the Olympic Dam Cu-U-Au deposit, South Australia: A geochemical tracer and reconnaissance Pb-Pb geochronometer: Precambrian Research, v. 238, p. 129–147, https://doi.org/10.1016/j.precamres.2013.10.007.

Courtney-Davies, L., Ciobanu, C.L., Tapster, S.R., Cook, N.J., Ehrig, K., Crowley, J.L., Verdugo-Ihl, M.R., Wade, B.P., and Condon, D.J., 2020, Opening the magmatic-hydrothermal window: High-precision U-Pb geochronology of the Mesoproterozoic Olympic Dam Cu-Au-Ag deposit, South Australia: Economic Geology and the Bulletin of the Society of Economic Geologists, v. 115, p. 1855–1870, https://doi.org/10.5382/econgeo.4772.

Drexel, J.F., Preiss, W.V., and Parker, A.J., 1993, The Geology of South Australia, Volume 1: The Precambrian: Geological Survey of South Australia Bulletin 54, 242 p.

Ehrig, K., McPhie, J., and Kamenetsky, V., 2012, Geology and mineralogical zonation of the Olympic Dam iron oxide Cu-U-Au-Ag deposit, South Australia, *in* Hedenquist, J.W., et al., eds., Geology and Genesis of Major Copper Deposits and Districts of the World: A Tribute to Richard H. Sillitoe: Society of Economic Geologists Special Publication 16, p. 237–267, https://doi.org/10.5382/SP.16.11.

Ehrig, K., Macmillan, E., Kamenetsky, V.S., Kamenetsky, M., McPhie, J., Thompson, J., Ciobanu, C., Cook, N., and Maas, R., 2018, Uraninite age dating: Multiple stages of uranium precipitation at Olympic Dam: Proceedings of the AusIMM International Uranium Conference, Adelaide, 5–6 June 2018, abstract number 20.

Fayek, M., Janeczek, J., and Ewing, R.C., 1997, Mineral chemistry and oxygen isotopic analyses of uraninite, pitchblende and uranium alteration minerals from the Cigar Lake deposit, Saskatchewan, Canada: Applied Geochemistry, v. 12, p. 549–565, https://doi.org/10.1016/S0883-2927(97)00032-2.

Frimmel, H.E., Schedel, S., and Brätz, H., 2014, Uraninite chemistry as forensic tool for provenance analysis: Applied Geochemistry, v. 48, p. 104–121, https://doi.org/10.1016/j.apgeochem.2014.07.013.

Fryer, B.J., and Taylor, R.P., 1987, Rare-earth element distributions in uraninites: Implications for ore genesis: Chemical Geology, v. 63, p. 101–108, https://doi.org/10.1016/0009-2541(87)90077-5.

Gulson, B.L., and Mizon, K.J., 1980, Lead isotope studies at Jabiluka, *in* Ferguson, J., and Goleby, A.B., eds., Uranium in the Pine Creek Geosyncline: Vienna, International Atomic Energy Agency, p. 439–456.

Hitzman, M.W., Oreskes, N., and Einaudi, M.T., 1992, Geological characteristics and tectonic setting of Proterozoic iron-oxide (Cu-U-Au-REE) deposits: Precambrian Research, v. 58, p. 241–287, https://doi.org/10.1016/0301-9268(92)90121-4.

Hoffman, P.F., et al., 2017, Snowball Earth climate dynamics and Cryogenian geology-geobiology: Science Advances, v. 3, e1600983, https://doi.org/10.1126/sciadv.1600983.

Johnson, J.P., 1993, The geochronology and radiogenic isotope systematics of the Olympic Dam copper-uranium-gold-silver deposit, South Australia [Ph.D. thesis]: Canberra, Australian National University, 251 p.

Johnson, J.P., and Cross, K.C., 1995, U-Pb geochronological constraints on the genesis of the Olympic Dam Cu-U-Au-Ag deposit, South Australia: Economic Geology and the Bulletin of the Society of Economic Geologists, v. 90, p. 1046–1063, https://doi.org/10.2113/gsecongeo.90.5.1046.

Kirchenbaur, M., Maas, R., Ehrig, K., Kamenetsky, V.S., Strub, E., Ballhaus, C., and Münker, C., 2016, Uranium and Sm isotope studies of the supergiant Olympic Dam Cu-Au-U-Ag deposit, South Australia: Geochimica et Cosmochimica Acta, v. 180, p. 15–32, https://doi.org/10.1016/j.gca.2016.01.035.

Kister, P., Cuney, M., Golubev, V.N., Royer, J.-J., Le Carlier De Veslud, C., and Rippert, J.-C., 2004, Radiogenic lead mobility in the Shea Creek unconformity-related uranium deposit (Saskatchewan, Canada): Migration pathways and Pb loss quantification: Comptes Rendus Geoscience, v. 336, p. 205–215, https://doi.org/10.1016/j.crte.2003.11.006.

Li, Z.X., et al., 2008, Assembly, configuration, and break-up history of Rodinia: A synthesis: Precambrian Research, v. 160, p. 179–210, https://doi.org/10.1016/j.precamres.2007.04.021.

Lyons, T.W., Reinhard, C.T., and Planavsky, N.J., 2014, The rise of oxygen in Earth's early ocean and atmosphere: Nature, v. 506, p. 307–315, https://doi.org/10.1038/nature13068.

Maas, R., Apukhtina, O.B., Kamenetsky, V.S., Ehrig, K., Sprung, P., and Münker, C., 2020, Carbonates at the supergiant Olympic Dam Cu-U-Au-Ag deposit, South Australia part 2: Sm-Nd, Lu-Hf and Sr-Pb isotope constraints on the chronology of carbonate deposition: Ore Geology Reviews, 103745, https://doi.org/10.1016/j.oregeorev.2020.103745 (in press).

Macmillan, E., Ciobanu, C.L., Ehrig, K., Cook, N.J., and Pring, A., 2016a, Chemical zoning and lattice distortion in uraninite from Olympic Dam, South Australia: American Mineralogist, v. 101, p. 2351–2354, https://doi.org/10.2138/am-2016-5753.

Macmillan, E., Cook, N.J., Ehrig, K., Ciobanu, C.L., and Pring, A., 2016b, Uraninite from the Olympic Dam IOCG-U-Ag deposit: Linking textural and compositional variation to temporal evolution: American Mineralogist, v. 101, p. 1295–1320, https://doi.org/10.2138/am-2016-5411.

Martz, P., Mercadier, J., Perret, J., Villeneuve, J., Deloule, E., Cathelineau, M., Quirt, D., Doney, A., and Ledru, P., 2019, Post-crystallization alteration of natural uraninites: Implications for dating, tracing, and nuclear forensics: Geochimica et Cosmochimica Acta, v. 249, p. 138–159, https://doi.org/10.1016/j.gca.2019.01.025.

McPhie, J., Kamenetsky, V., Allen, S., Ehrig, K., Agangi, A., and Bath, A., 2011a, The fluorine link between a supergiant ore deposit and a silicic large igneous province: Geology, v. 39, p. 1003–1006, https://doi.org/10.1130/G32205.1.

McPhie, J., Kamenetsky, V.S., Chambefort, I., Ehrig, K., and Green, N., 2011b, Origin of the supergiant Olympic Dam Cu-U-Au-Ag deposit, South Australia: Was a sedimentary basin involved?: Geology, v. 39, p. 795–798, https://doi.org/10.1130/G31952.1.

Oreskes, N., and Einaudi, M.T., 1990, Origin of rare earth element-enriched hematite breccias at the Olympic-Dam Cu-U-Au-Ag deposit, Roxby Downs, South Australia: Economic Geology and the Bulletin of the Society of Economic Geologists, v. 85, p. 1–28, https://doi.org/10.2113/gsecongeo.85.1.1.

Reeve, J.S., Cross, K.C., Smith, R.N., and Oreskes, N., 1990, Olympic Dam copper-uranium-gold-silver deposit, *in* Hughes, F.E., ed., Geology of the Mineral Deposits of Australia and Papua New Guinea: Australasian Institute of Mining and Metallurgy Monograph 14, p. 1009–1035.

Tonkin, D.G., and Creelman, R.A., 1990, Mount Gunson copper deposits, *in* Hughes, F.E., ed., Geology of the Mineral Deposits of Australia and Papua New Guinea: Australasian Institute of Mining and Metallurgy Monograph 14, p. 1037–1043.

Trueman, N.A., Long, J.V.P., Reed, S.J.B., and Chinner, G.A., 1986, The lead-uranium systematics, and rare earth element distributions of some Olympic Dam and Stuart Shelf mineralisation: Adelaide, Australia, Western Mining Corporation, Olympic Dam Geology Report 99.

Trueman, N.A., Long, J.V.P., Reed, S.J.B., and Chinner, G.A., 1988, The lead-uranium systematics, and rare earth element distributions of some Olympic Dam and Stuart Shelf mineralisation: Adelaide, Australia, Western Mining Corporation, Olympic Dam Geology Report 143.

Veevers, J.J., 2004, Gondwanaland from 650–500 Ma assembly through 320 Ma merger in Pangea to 185–100 Ma breakup: Supercontinental tectonics via stratigraphy and radiometric dating: Earth-Science Reviews, v. 68, p. 1–132, https://doi.org/10.1016/j.earscirev.2004.05.002.

Printed in USA